Development and Validation of a Compact Thermal Model for an Aircraft Compartment

Geron, M., Butler, C., Stafford, J., & Newport, D. (2013). Development and Validation of a Compact Thermal Model for an Aircraft Compartment. *Applied Thermal Engineering*, *61*(2), 65–74. https://doi.org/10.1016/j.applthermaleng.2013.07.012

Published in:
Applied Thermal Engineering

Document Version:
Peer reviewed version

Queen's University Belfast - Research Portal:
Link to publication record in Queen's University Belfast Research Portal

Accepted Manuscript

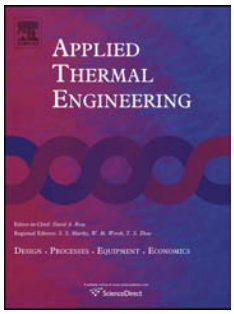

Development and Validation of a Compact Thermal Model for an Aircraft Compartment

M. Geron, C. Butler, J. Stafford, D. Newport

PII: S1359-4311(13)00500-0

DOI: 10.1016/j.applthermaleng.2013.07.012

Reference: ATE 4926

To appear in: *Applied Thermal Engineering*

Received Date: 5 December 2012

Revised Date: 3 July 2013

Accepted Date: 7 July 2013

Please cite this article as: M. Geron, C. Butler, J. Stafford , D. Newport, Development and Validation of a Compact Thermal Model for an Aircraft Compartment, *Applied Thermal Engineering* (2013), doi: 10.1016/j.applthermaleng.2013.07.012.

Highlights

- Development of a reduced order model for the case of an aircraft crown compartment
- A thermal fluid network is generated for its mixed convection regime
- Regression analysis utilised to evaluate characteristic parameters
- The thermal fluid network is simple but its accuracy is close to the detailed model

Development and Validation of a Compact Thermal Model for an Aircraft Compartment

M. Geron[a], C. Butler[b], J. Stafford[c], D. Newport[b,*]

[a] *National University of Ireland Galway, Galway, Ireland*
[b] *Stokes Institute, University of Limerick, Limerick, Ireland*
[c] *Bell Labs, Alcatel-Lucent, Dublin, Ireland*

Abstract

The development of accurate structural/thermal numerical models of complex systems, such as aircraft fuselage barrels, is often limited and determined by the smallest scales that need to be modelled. The development of reduced order models of the smallest scales and consequently their integration with higher level models can be a way to minimise the bottle neck present, while still having efficient, robust and accurate numerical models. In this paper a methodology on how to develop Compact Thermal Fluid Models (CTFMs) for compartments where mixed convection regimes are present is demonstrated. Detailed numerical simulations (CFD) have been developed for an aircraft crown compartment and validated against experimental data obtained from a 1:1 scale compartment rig. The crown compartment is defined as the confined area between the upper fuselage and the passenger cabin in a single aisle commercial aircraft. CFD results were utilised to extract average quantities (temperature and heat fluxes) and characteristic parameters (heat transfer coefficients) to generate CTFMs. The CTFMs have then been compared with the results obtained from the detailed models showing average errors for temperature predictions lower than 5%. This error can be deemed acceptable when compared to the nominal experimental error associated with the thermocouple measurements.

The CTFMs methodology developed allows to generate accurate reduced

*Corresponding author
Email address: david.newport@ul.ie (D. Newport)

order models where accuracy is restricted to the region of Boundary Conditions applied. This limitation arises from the sensitivity of the internal flow structures to the applied boundary condition set. CTFMs thus generated can be then integrated in complex numerical modelling of whole fuselage sections.

Further steps in the development of an exhaustive methodology would be the implementation of a logic ruled based approach to extract directly from the CFD simulations numbers and positions of the nodes for the CTFM.

Keywords: Heat transfer, CFD, Reduced order models, Aircraft compartment

1. Introduction

The thermal analysis of complex systems (e.g. aircraft fuselage barrel) requires the solutions of different spatial scales. Numerical methods such as CFD are constrained by the smallest scales that need to be solved. Even with the increment in computer power witnessed in the last two decades, these methods are still too slow or unfeasible for full scale simulations. This issue is particularly relevant in the design phase where the effect of different parameters and their interaction needs to be addressed. The development of reduced order models (ROMs) can allow for the finding of the compromise between accuracy required and complexity of the model.

Reduced order models may thus be used in conjunction with optimisation routines, to quickly perform parameter sensitivity studies, or be integrated with multi-scale computations to efficiently bridge a range of length scales. ROMs can be distinguished into two different categories depending on the approach: a state space model in which the problem is divided into input and output, and a distributed parameter [1].

The fundamental principle for distributed parameter modelling is the search for a suitable set of modes on which to project the governing equations onto, reducing the solution procedure to find the appropriate weight coefficients that combine the modes into the desired approximate solution. These are typically proper orthogonal decomposition methods which have been applied to different

cases [2, 3, 4].

In the category of state space models it is possible to allocate Compact Thermal Models (CTMs) and Flow Network Models (FNMs). CTMs have been successfully employed in the analysis and development of electronic components where the conductivity of the materials was unknown. The DELPHI team [5, 6] developed a formal procedure to generate CTMs which were Boundary Condition Independent. In this way the CTMs were reproducing the object behaviour under "any" boundary condition applied and could be used as a black box. The procedure consisted firstly, in the definition of a set of boundary conditions of interest, and secondly in the evaluation of the resistances, which characterise the CTM, through the minimisation of a cost function. Sabry and Bosch [7, 8, 9] developed matricial calculus to better define and characterise CTMs and the boundary condition independence hypothesis. CTMs were also applied in scenarios where convective heat transfer was present. In these cases correlations have been utilised to define the heat transfer resistance. Sabry [10] also developed a generalised definition of heat transfer coefficient and formalised its utilisation in system simulations. The model presented, quite promising for 2D pipe flow applications, still needs further studies to be implemented in more complex systems.

For problems of natural and mixed convections, where velocity scales and thermal scales are of the same order of magnitude, the values of the conductors (heat transfer coefficient in this case) may strongly depend on the boundary conditions applied. For this configuration an integration of thermal and fluid models must be applied. Miana et al. [11, 12] developed a formal procedure and showed the results of a combination of thermal network modelling and flow network modelling for an electronic control unit of an automobile.

In this paper a comprehensive strategy for developing a CTFM for an aircraft fuselage confined compartments (e.g crown compartment), in which both natural and forced convection are relevant, is investigated. A detailed model of the crown compartment is developed in FLUENT and compared against experimental data. The commercial package SINDA/FLUINT is utilised to generate

compact thermal fluid models. Results of the CTFMs are then compared against the outputs of the detailed simulations.

Nomenclature

a	area	(m^2)
D	numerical domain dimension	(-)
F_s	GCI safety factor	(-)
f	grid solution variable	(-)
h	heat transfer coefficient	(W/m^2 K)
l	length	(m)
N	number of grid nodes	(-)
p	numerical method order of accurarcy	(-)
Q	heat rate	(W)
R	thermal resistance	(m^2K/W)
R^2	coefficient of determination	(-)
r	grid refinement factor	(-)
T	temperature	(K)
V	velocity	(m/s)
Ω	node	(-)

Abbreviations

BCI	Boundary Condition Independence
GCI	Grid Convergernce Index
CTM	Compact Thermal Model
CTFM	Compact Thermal Fluid Model
CFD	Computational Fluid Dynamics

Subscripts

amb	ambient
avg	average
$coarse$	coarse grid
$fine$	fine grid
$floor$	average floor value
fus	fuselage
i	i-node
in	inlet
out	outlet

2. The aircraft crown compartment

The crown compartment is one of the confined compartments present in an aircraft fuselage as sketched in figure 1. It is delimited by the external skin of the fuselage and the cabin roof. The crown compartment is characterised by a single layer of insulation along the fuselage and a double layer of insulation along the cabin roof. A mass flow rate due to the air conditioning in the cabin is also present. Several dissipating elements, such as lights, power cables, power supplies and avionic components can be located in this compartment.

Due to its complexity only an unpopulated crown compartment has been analysed in this study. This choice even if limiting, was consequence of the desire to analyse a solid methodology to develop CTFM, concentrating more on the effects of varying boundary conditions (i.e mass flow rate and fuselage temperature) in a CTFM without introducing the complexity of dissipating elements. This also gave the possibility to verify the detailed simulations (CFD) versus experimental data obtained from an experimental crown compartment rig.

2.1. Experimental set up

Shown in figure 2 is the crown compartment experimental test facility built at the University of Limerick. The test rig is a full scale model of a crown

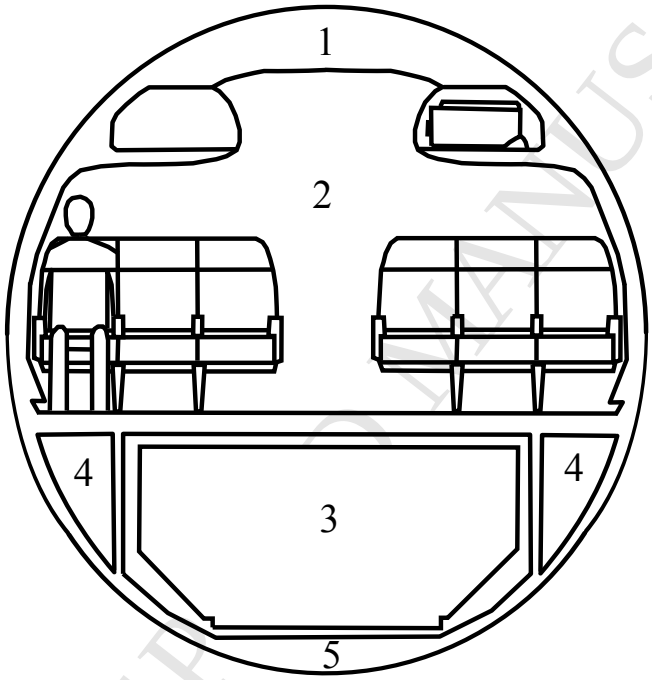

Figure 1: Cross section of single aisle aircraft fuselage 1) Crown ; 2) Cabin; 3) Cargo bay; 4) Triangle; 5) Bilge

compartment with the test cavity's major external dimensions of 2.45m × 0.4m × 1.17m (width × height × depth). The inlet for the ventilation into the cavity was located on the floor of the compartment at the vertical centreline. The inlet is 40mm wide. The air from the ventilation system enters through this inlet and exits through the two outlets at either side of the compartment. The two outlets are 20mm wide and are also located on the floor. The fuselage section and floor of the compartment were manufactured from 6mm polycarbonate (Marlon FS). The solar load on the fuselage was reproduced with an array of 12 PID controlled heater mats. The mass flow rate of the ventilation into the compartment was generated with a bank of 10 EBM PAPST 412F 12Vdc axial fans. The internal surface of the fuselage was insulated with 50mm insulation with a thermal conductivity of 0.057W/m.K. The crown floor was also insulated with 100mm of insulation to reduce heat loss. The front and back walls of the compartment consisted of triple-glazed panels. This was to allow for optical access inside the compartment.

For each test, the fuselage temperature was set on the PID controllers and the mass flow rate regulated by adjusting the power to the fans. Temperatures were recorded every minute using 26 K-type thermocouples connected to an Agilent 34970A data logging system located in the positions represented by the green dots in figure 2. It took approximately 6 hours to reach steady state. Steady state was defined as a change of less than 0.2K/hr. A first batch of tests was conducted considering fuselage temperatures of 323K, 348K and 378K and a mass flow rate of 7.8g/s. The higher temperature is representative of Hot Day conditions where the external skin of the aircraft can reach quite high temperatures. The thermocouples had been calibrated in a Lauda Ecoline Star-edition Re103 water bath prior to fixing them to the test rig. The associated measurement uncertainty was 0.2K.

2.2. Numerical Setup

The bi-dimensional numerical domain considered comprises of the whole mid section of the crown compartment and its dimensions are the same as the

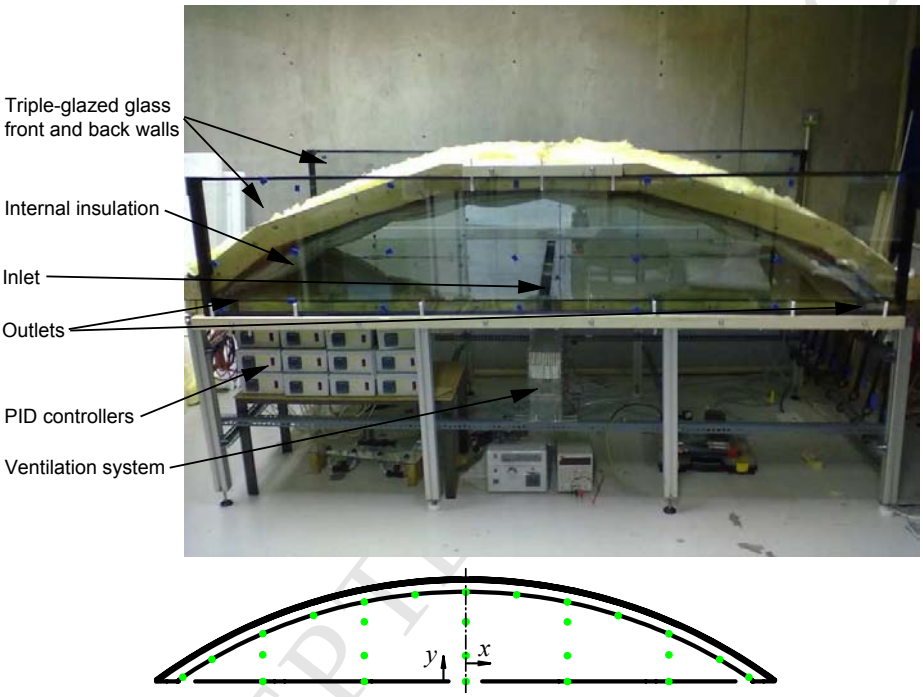

Figure 2: Experimental set-up in the laboratory and the positions of the thermocouples represented by green dots

experimental rig. The geometric symmetry which exists for the unpopulated crown compartment has not been considered in the definition of the numerical domain. This was due to small differences in temperature profiles that were identified when numerical simulations were run for the whole compartment and for its half.

The domain is composed of a solid zone (insulation) and of a fluid zone, whose properties are reported in table 1. The fluid zone was modelled as an incompressible ideal gas. The present study only considers dry air, appropriate for hot dry climates, but moisture content can be present in the air in application arising either from the local environment, and the presence of passengers in the cabin from which air is drawn into the crown compartment. Laguerre et al. [13] performed an experimental and numerical study of heat and moisture content in a cavity representative of a refrigerator. They noted when comparing the dry with humid, that the presence of water evaporation and condensation leads to an increase in air velocity. This is consistent with Zhang et al. [14] who examined the sensitivity of natural convection heat transfer coefficients to relative humidity. McBain [15] examined the scaling of flow in a differentially heated square cavity and states that the humidity transport equation can be neglected if the air is saturated everywhere. The Prandtl number and the thermophysical properties must then be modified to account for the moisture content. The presence of moisture will influence radiative exchange whereby the fluid will have a lower transmissibility, effectively increasing the thermal transport to the fluid. Coupled with the high specific heat capacity and conductivity of water relative to air, improved thermal transport due to moisture should be expected. In accounting for thermal transport under Hot Day conditions, the dry air scenario examined provides a conservative representation.

The Reynolds Averaged Navier-Stokes (RANS) formulation was chosen to describe the equations of motion for the fluid. To solve the closure problem which arises with this formulation of the Navier-Stokes equations, the RNG $k - \varepsilon$ turbulent model was adopted in this study. Radiation heat exchange was also modelled. Because dry air was the working fluid with minimal carbon

Table 1: Material Properties

Material/Properties	Insulation	Polycarbonate	Air
Density$[kg/m^3]$	180	1300	*Incompressible Ideal Gas* ($\rho = P/RT$)
Specific Heat $[J/kg \cdot K]$	840	1200	1004
Conductivity$[W/m \cdot K]$	0.057	0.2	0.0257

dioxide content, the medium was deemed as non participating and a surface to surface (S2S) radiation model was adopted. All simulations were considered at steady state.

All the walls present (fuselage and cabin roof) have been considered made of polycarbonate in accordance with the material used for the test rig manufactured. Polycarbonate serves as a good thermal representation of carbon fibre used for aircraft fuselages due to similar thermal properties.

2.2.1. Boundary conditions

The type of boundary conditions applied were as follows: a constant temperature profile was applied along the fuselage and an adiabatic wall condition has been defined for the cabin roof. For the part of the insulation directly in contact with the fluid, a "coupled boundary condition" has been applied. In this way the thermal balance along the surface will be the equilibrium between the heat dissipated into the fluid, and the heat coming from the fuselage. A constant velocity inlet profile has been applied at the inlet section, while a pressure outlet condition has been applied at the two outlet sections.

2.2.2. Mesh

The grid utilised to discretise the numerical domain consisted of a multi block mesh with structured and unstructured distribution of the cells and it has been reported in figure 3. A structured quadrilateral mesh was utilised for the central part of the compartment, while an unstructured triangular mesh was utilised for the two corners. Eventually an unstructured quadrilateral mesh was utilised for the discretisation of the insulation part. The fluid mesh consisted of 12253 cells while the insulation part comprised of 2590 cells. A denser cell distribution has been used at the walls in order to better resolve the fluid and

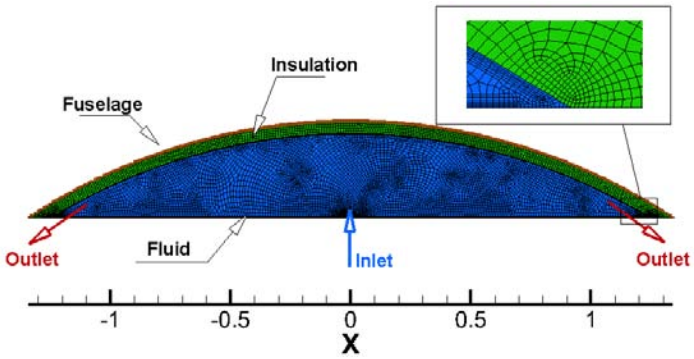

Figure 3: Mesh of the crown compartment

thermal boundary layer which develop along the walls.

In order to deem the results obtained grid independent, a grid convergence analysis has been carried out. Two different grids, belonging to the same family have been generated. The refinement factor r, for the two grids, was equal to 1.3. The refinement factor is defined as $r = (N_{fine}/N_{coarse})^{1/D}$ where N_{fine} is the number of nodes in the fine mesh, N_{coarse} the number of nodes in the coarse mesh and D the numerical domain dimension. A refinement value $r \geq 1.3$ is defined by Roache [16] as the minimum value to carry out a grid convergence analysis. The coarse grid was composed of 11413 nodes and the fine grid of 14843 nodes. A qualitative comparison between the results obtained with the two grids is reported in figure 4 a), b) and c). In the figure a comparison between the temperature profiles is carried out at three vertical sections (x=0m, x=0.4m and x=0.8m). Some discrepancy between the fine and coarse grid can been seen especially in zones of stratified flows where velocity gradients are quite small. These zones are usually quite difficult to capture with numerical methods. In general the two solutions obtained with the coarse grid and fine grid are quite close suggesting an independence of the solution from the grid resolution.

To estimate the band of error associated with the fine grid, the Grid Convergence Index (GCI) introduced by Roache [16] has been utilised. The GCI

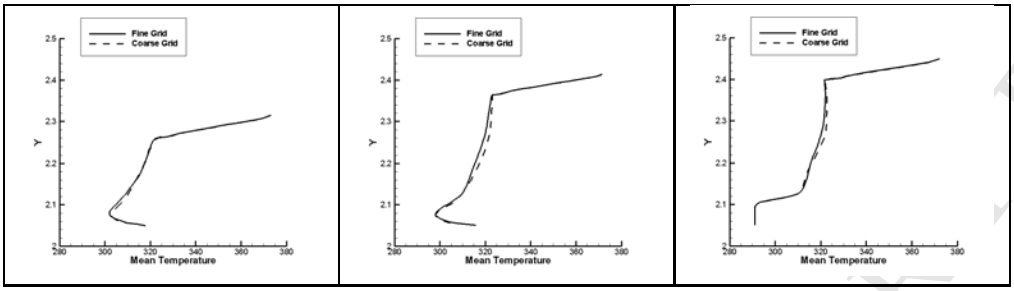

a) Section x=-0.8m	b) section x=-0.4m	c) section x=0m

Figure 4: Grid independence analysis along three vertical sections

Table 2: Grid convergence analysis

	Avg ins.Temp.	Heat Flux	Rad. Heat Flux	Avg. Fluid Temp
	[K]	[W/m^2]	[W/m^2]	[K]
f_1	321.8	51.74	31.43	313.3
f_2	321.5	51.72	31.36	313.7
ε	0.00072	0.00045	0.0022	-0.0012
GCI	0.315%	0.196%	0.96%	0.55%

is based on generalized Richardson Extrapolation [17] involving comparison of discrete solutions at two different grid spacings. The GCI is defined as

$$GCI = F_s \left| \frac{\varepsilon}{r^p - 1} \right| \tag{1}$$

where $\varepsilon = (f_1 - f_2)/f_1$, and where f_1 represents a fine grid numerical solution, f_2 a coarse grid numerical solution and $p = 2$ the actual formal order of accuracy of the numerical method. F_s is a security factor equal to 3 in the case of two grids. The GCI was thus evaluated considering four different parameters which will be of interest in the development of CFTMs: the average temperature of the insulation, the average heat flux and the average radiative heat flux at the insulation and the average fluid temperature. The values evaluated are reported in table 2.

The low values of the GCI, which can be seen as an error estimator, assure that the solutions obtained in the fine grid are affected by a numerical error lower than 1% which is sufficiently small for this study.

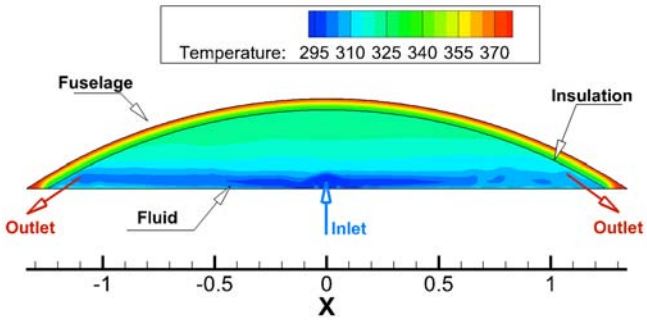

Figure 5: Numerical solution of the unpopulated crown compartment for $T_{fus} = 378.15$K

2.2.3. Numerical Solutions

A typical result obtained for the crown domain previously described is illustrated in figure 5. It is possible to distinguish two different fluid zones: a bottom zone characterised by forced convection and a top zone characterised by stratified fluid. In the bottom zone, the fluid that enters into the compartment due to the air conditioning system, does not have the necessary momentum to reach the top of the compartment and remains confined at the bottom of the crown before exiting from the two outlets. In the top zone however no coherent fluid motion is observable; the fluid appears stratified and heat transfer takes place through conduction along the fluid. Similar flow and heat patterns are observable for lower values of the fuselage temperature. The main difference consists of the height of the plume of the jet entering into the compartment. Higher fuselage temperatures decrease the momentum of the jet due to buoyancy effects.

2.2.4. Numerical solution Validation

A comparison of the experimental temperature data and the numerical prediction along the insulation surface is shown in figure 6. An overall good agreement could be verified. It is noticeable however that the numerical data present a flatter profile than the experiments. It is believed that the oscillations of the

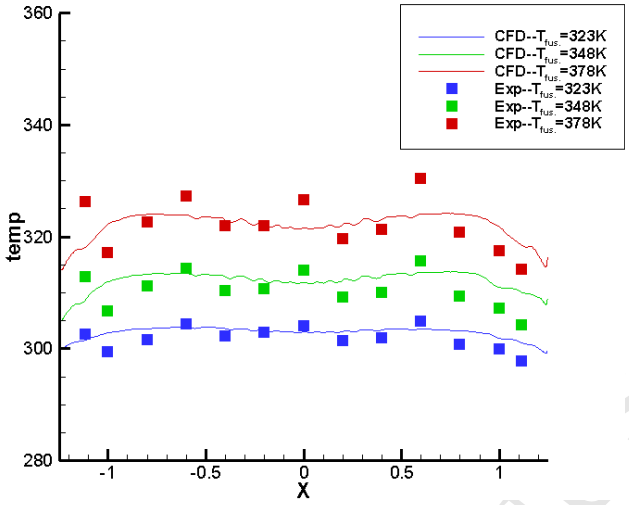

Figure 6: Comparison of CFD and Exp. data along the insulation surface

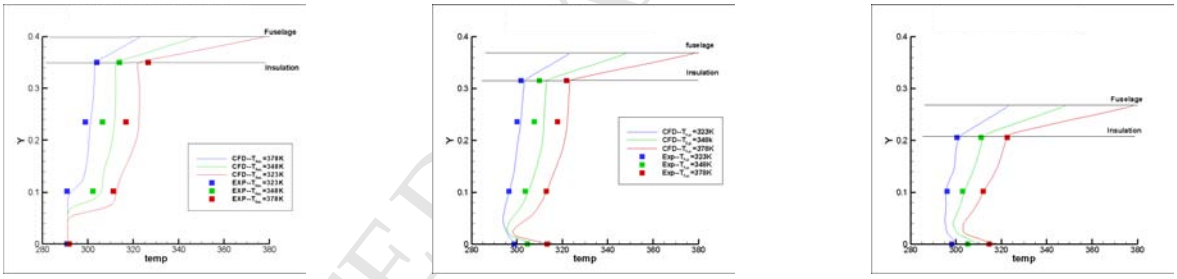

a) Temperature profiles at x=0m b) Temperature profiles at x=0.4m c) Temperature profiles at x=0.8m

Figure 7: Comparison CFD and Exp. data at three vertical locations

experimental data are a consequence of the way in which the insulation has been inserted in the crown compartment. The insulation was attached to the fuselage using pegs glued to the surface. This reproduces the way in which the insulation is attached in an actual crown compartment. In this way the insulation assumes a wavy profile, as it is possible to observe in figure 2, which is not reproduced in the numerical model and could be responsible for the temperature oscillations.

The comparison between the experimental data recorded along three vertical sections inside the compartment and the numerical simulations is shown in figure 7 a) b) and c). In general a good match is shown between numerical

and experimental data assuring the capability of the numerical simulations to predict the flow features and temperature gradients for an unpopulated crown compartment. The maximum relative error verified is around 1.76% while the minimum is lower than 0.1% with an overall average error smaller than 0.7%. It is also possible to notice from the graphs reported how the match tends to be quite good for the lower fuselage temperature case (blue lines) while it is inclined to decrease for higher temperature values (green and red lines). This could be the result of not reproducing the radiating heat transfer correctly due to the use of nominal emissivity value in the numerical simulations.

3. Reduced order models

3.1. Thermal Fluid Network Model

The principal aim of this research is to examine a robust procedure to develop CTFMs for confined compartments in a mixed convection regime. Outputs of interest for the CTFMs developed are the average temperature inside the compartment T_{avg} and the temperatures and heat rates along the insulation surface, under a specific set of boundary conditions.

The main steps in the development of CTFMs can be summarised as follow: firstly the domain is divided into nodes and lumps. Nodes and lumps can been seen as zones in the space (Ω_i) where quantities such as temperature (T_i) and heat rate (Q_i) are represented by their volume/area average value [8],

$$T_i = \frac{\int_{\Omega_i} T_i da}{\int_{\Omega_i} da};\; Q_i = \int_{\Omega_i} Q_i da \tag{2}$$

where da is the element area.

In thermal network models nodes exchange energy through conductors via radiation and conduction-convection. For fluid network models lumps and paths are defined. These are analogous to traditional thermal nodes and conductors, but are much more suited to fluid system modelling. Unlike thermal networks, fluid networks are in fact able to simultaneously conserve mass and momentum as well as energy [18].

Secondly a set of boundary conditions under which the CTFM must operate needs to be defined. In the DELPHI [5] methodology, CTMs were developed and optimised for a wide set of boundary conditions with the purpose of developing CTMs which could be deemed Boundary Condition Independent (BCI) and thus used as black boxes. However this approach is not fully reproducible when flow features and heat transfer depend tightly on the boundary conditions applied as happens with natural and mixed convection. Consequently, in order to develop a robust CTFM, the set of boundary conditions considered has been limited to the "operative conditions" of the crown compartment. Two input variables have thus been defined: the fuselage temperature, T_{fus}, and the mass flow rate that enters the compartment. The mass flow, which is constant for a specific fuselage section, varies significantly with the position of the section along the fuselage and for this reason it was deemed as an input parameter of interest.

The last step, in the development of CTFMs, consists of the evaluation of those parameters such as heat transfer coefficients and thermal conductivity that characterise the energy exchange between nodes. The specificity of the geometry, the unknown thermal properties of the actual insulation, and the mixed convection regime present in the compartment do not allow the use of standard correlations with much confidence. In this case it is preferable to extract some information directly from the CFD simulations.

In this project regression analysis techniques have been used to extract, from the CFD results, heat transfer coefficients which characterise the convection phenomena along the insulation surface under the set of boundary conditions specified. Other characteristic parameters where instead evaluated directly in the CTFM through the minimisation of a cost function such as the one reported in eq. (3).

$$F = \sqrt{\sum_{i=1}^{N} \left(T_{i_{CTM}} - T_{i_{CFD}}\right)^2} + \sqrt{\sum_{i=1}^{N} \left(Q_{i_{CTM}} - Q_{i_{CFD}}\right)^2} \tag{3}$$

The CTFM thus generated was then solved utilising the commercial software

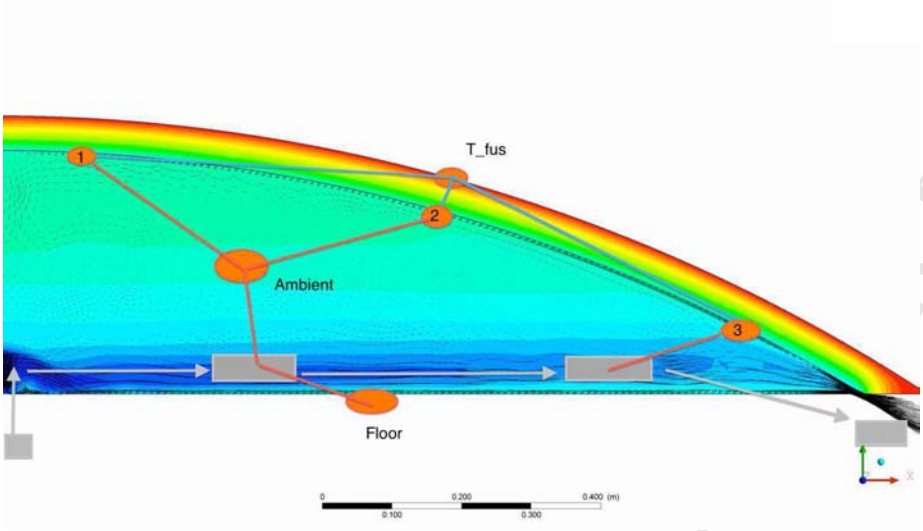

Figure 8: Schematic of compact thermal fluid model of a crown compartment

SINDA/FLUINT [19]. SINDA/FLUINT is an equation solver for CTFMs with built in capability to solve optimisation processes. This capability was utilised to evaluate thermal parameters which were not extracted from the CFD simulations through minimisation of the function in eq. (3). It is worth mentioning that as a difference from the DELPHI methodology, where a minimum value of the cost function was sought all over the set of boundary conditions applied, here the minimum was sought only for each boundary condition and then quadratically interpolated over the whole set of boundary conditions. The reason for the different strategy relies on the strongest link that thermal fluid models can have with the boundary conditions applied.

3.2. Specific problem

The CTFM developed, based on the flow features highlighted by the CFD simulations, consists of 6 nodes and 4 fluid lumps as shown in figure 8. One node Ω_{fus} was defined for the fuselage. Three nodes were defined along the insulation $(\Omega_1, \Omega_2, \Omega_3)$, and their space extensions were determined by analysing the temperature profiles and the heat transfer along the insulation surface obtained from the CFD simulations. In figure 9 temperature profiles, total heat

Table 3: Case studies

	T_{fus} (K)	V_{in} (m/s)
Case A	323.15	0.15
Case B	348.15	0.15
Case C	378.15	0.15

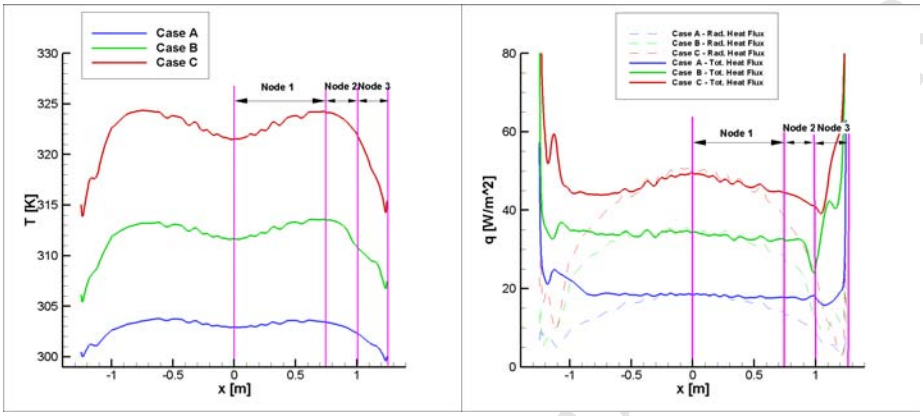

Figure 9: Temperature and heat flux along the insulation surface

transfer and radiation heat transfer are reported for three different cases defined in table 3 .

Thus Ω_1 was defined as the surface which is enclosed by the symmetry axis $x = 0$m and $x = 0.75$m, $\left(\Omega_1 = \int_0^{0.75} dl\right)$, node 2 as $\left(\Omega_2 = \int_{0.75}^{1} dl\right)$ and node 3 as $\left(\Omega_3 = \int_{1}^{1.25} dl\right)$.

One node, Ω_{amb}, was defined for the average temperature of the air inside the compartment. The last node defined, Ω_{floor}, is the node representing the floor of the compartment. Four lump nodes were utilised to describe the flow confined at the bottom of the compartment. The lumped nodes where characterised by defining the mass flow rate from the inlet velocity V_{in}, and the inlet temperature. It was assumed that the the fuselage temperature range was between 323K $\leq$ $T_{fus} \leq$ 378K, while the velocity ranges from $0.6m/s \leq V_{in} \leq 0.22m/s$. The inlet temperature was kept constant at $T_{in} = 298.15$K. Pressure drops were not modelled with this ROM because of the small interest for this specific case.

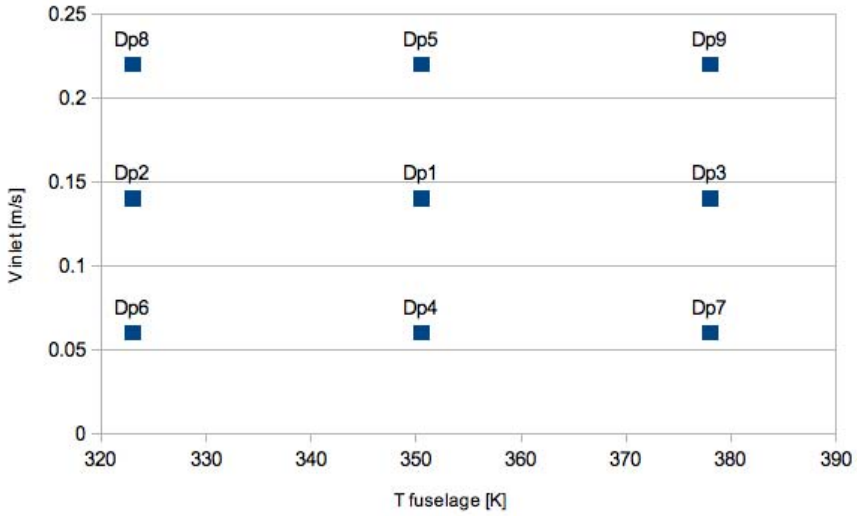

Figure 10: Design points for central composite design

3.2.1. Coefficient evaluation

As previously outlined, for this non typical compartment, correlations for the heat transfer coefficient are not available. The heat transfer coefficients (h_1, h_2, h_3), which characterise the energy exchange of the three nodes $(\Omega_1, \Omega_2, \Omega_3)$ with the ambient node (Ω_{amb}) were thus evaluated from the CFD simulations utilising regression analysis techniques.

To evaluate the design points which will be used for the regression analysis a typical central composite design approach was chosen [20]. With this method each independent variable is chosen at the two boundaries (-1,+1) and at the middle point (0); the overall number of runs necessary will thus be 3^n where n is the number of independent variables. The fuselage temperature and the inlet velocity were selected as the independent variables for this case. The heat transfer coefficients for nodes 1, 2 and 3 (h_1, h_2, h_3) as well as the average temperature inside the compartment T_{avg} and the average floor temperature T_{floor} are the output variables of interest. The overall design points that will be utilised in the regression analysis are graphically reported in figure 10.

Table 4: Goodness of fit

Output Parameters	Coefficient of determination R^2
h_1	0.948
h_2	0.921
h_3	0.924
T_{avg}	0.998
T_{floor}	0.999

Table 5: Regression coefficients for output parameters extracted from CFD

	T_{fus}	V_{in}	T_{fus}^2	$T_{fus} \cdot V_{in}$	V_{in}^2	-
T_{avg}	8.089833	-5.386833	0.0652	-2.047	1.3071	306.86
T_{floor}	8.811833	-4.821167	0.07	-2.0335	1.2035	309.30
h_1	0.096393	0.20217	0.0547	-0.0860	0.0109	0.0692
h_2	0.29273	0.67084	0.2115	-0.4438	0.1754	1.151
h_3	0.029313	0.48722	0.2623	0.05428	0.4245	1.495

The coefficients for the quadratic expression of the response surfaces evaluated are reported in table 5. The "goodness of the fit" of the function thus determined is analysed through the coefficient of determination. The coefficient of determination (R^2) represents the percent of the variation of the output parameter that can be explained by the response surface regression equation. If no variation is present the coefficient is equal to 1. In table 4 the R^2 has been reported for each output variable.

The coefficient of determination is quite good for all the output parameters with a minimum value of 0.921 for h_2 and a maximum value of 0.999 for T_{floor} indicating a good correlation between input and output parameters.

To gain a better insight in the thermal behaviour of the output parameters from the input parameters, a sensitivity study has also been carried out and reported in the two figures 11 and 12.

The sensitivity for T_{avg} and T_{floor} from the input parameters is quite similar (figure 11). The input factors with the most influence are T_{fus} and V_{in}. The second order terms are not as influential as the first order, with near independence from T_{fus}^2. The factors $(T_{fus} \cdot V_{in})$ and V_{in}^2 have an influence of the same order of magnitude but in opposite direction. The dependence of the three heat transfer coefficients from the input parameters is slightly different (figure 12). The inlet velocity is the factor which influences the three output factors the

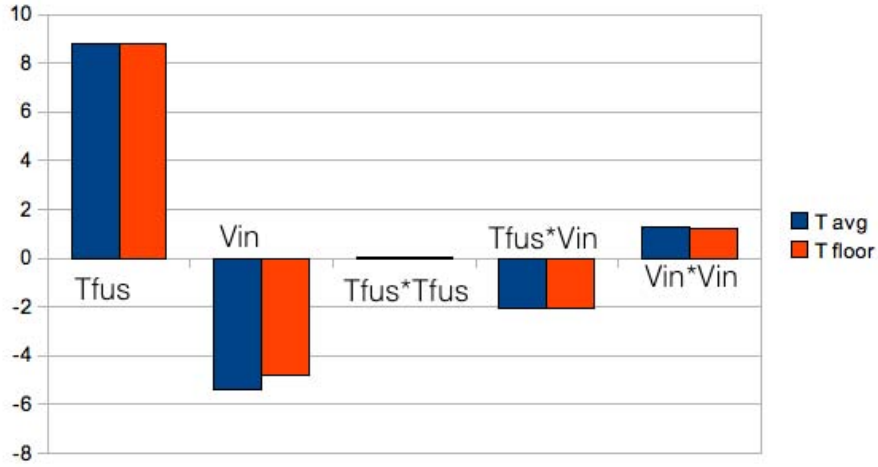

Figure 11: Sensitivity analysis of T_{avg} and T_{floor} to the input parameters

most. The heat transfer coefficient of node 3 shows a really low dependence from the fuselage temperature but a strong dependence from V_{in} and V_{in}^2 in accordance with what the CFD simulations were showing. This part of the insulation exchanges heat mainly with the cold flow coming from the cabin. The dependence of the output factors from the second order factors is more relevant for node 2 and 3 showing for h_1 an almost linear behaviour.

3.3. Compact Fluid Thermal Model

The CTFM formerly sketched has been implemented and solved in SINDA/FLUINT software as reported in figure 13. The ROM developed is a combination of thermal and fluid nodes and take into considerations the three different ways of heat exchange inside the compartment: radiative, convective and conductive heat transfer.

The radiative heat transfer has been considered only from surface to surface in accordance with the CFD simulations where the medium was regarded as non participating. The view factors necessary to define the radiative heat transfer were evaluated directly from the CFD. Ansys FLUENT [21] provides an internal subroutine which evaluates the view factors between any two surfaces. The radiative exchange has been represented in figure 13 as dashed-dot-dot lines.

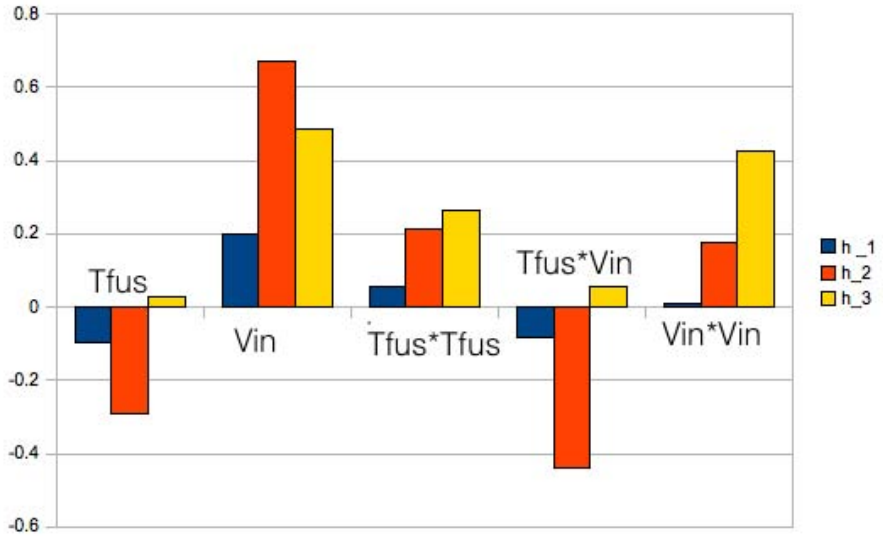

Figure 12: Sensitivity analysis of heat transfer coefficient (h_1, h_2, h_3) to the input parameters

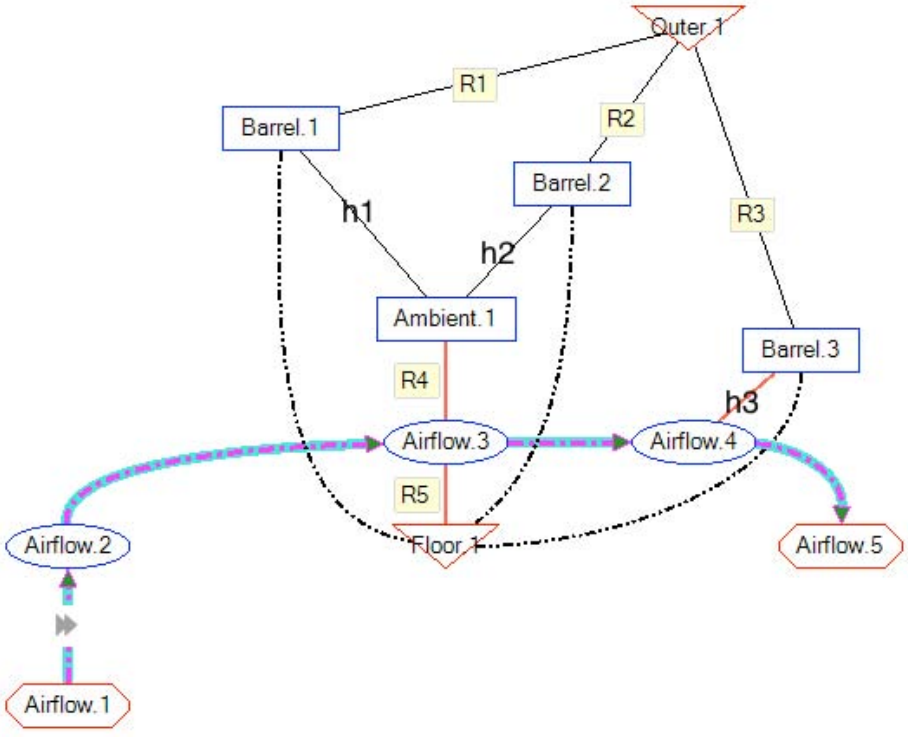

Figure 13: Compact thermal model schematic

Table 6: CTFM resistances

$R1$	$R2$	$R3$	$R4$	$R5$
1.457	4.317	3.466	see table 7	see table 7

Table 7: Regression coefficients for resistance $R4$ and $R5$

	T_{fus}	V_{in}	T_{fus}^2	$T_{fud} \cdot V_{in}$	V_{in}^2	-
R4	-1.3427	-1.3526	-1.7512	-0.5258	1.1203	5.7389
R5	-0.4665	-0.4929	0.3887	-0.1179	-0.1619	1.2394

The thermal resistance $R1$,$R2$,$R3$ as well as $R4$ and $R5$ which characterise the energy exchange between the different nodes, have been evaluated through the minimisation of the cost function formerly introduced (see eq. 3). A constant value has been found for $R1$,$R2$, and $R3$ (see table 6) for all the boundary conditions applied, depending only on the characteristics of the insulation material.

The values of $R4$ and $R5$, which minimise the cost function, change instead depending on the set of boundary conditions applied. Regression analysis has been applied to evaluate the functions to be utilised in the reduced order models for the two resistances. The coefficients of these functions are reported in table 7.

The comparison between the results obtained from the CTFMs and the CFD for the nine design points formerly introduced (see figure 10) has been reported in table 8. The error for the temperature has been defined as $(T_{CTFM} - T_{CFD})/(T_{CFD} - T_{in})$ where T_{in} is the temperature of the air coming from the cabin which is constant ($T_{in} = 298.15$K). The maximum temperature error recorded is on node 3 (design point 5) and equal approximately to 23% (1.85°C). The average error for nodes Ω_1 and Ω_2 is around 4% (0.5 °C) while reaches 8% for node Ω_3. Such small temperature differences between the predicted temperatures with the reduced order model and to those temperature foreseen by the CFD model allow confidence that the reduced model accurately simulates the thermal behaviour of the confined compartment.

The computational efficiency of the approach developed can also be demonstrated considering that the CPU hours ratio between the CTFMs simulation

Table 8: Comparison of CTFMs vs CFD

	Temperature (K)								
	Ω_1			Ω_2			Ω_3		
	CTFM	CFD	err%	CTF	CFD	err%	CTFM	CFD	err%
1	313.78	313.601	-1.16	314.27	313.866	-2.57	310.58	309.868	-6.08
2	303.124	303.856	12.83	303.102	303.748	11.54	301.36	301.768	11.28
3	324.23	323.809	-1.64	324.99	324.386	-2.30	319.73	319.422	-1.45
4	319.1	318.431	-3.30	319.85	320.226	1.70	317.13	318.268	5.64
5	310.5	310.791	2.30	310.23	309.857	-3.19	308.05	306.196	-23.04
6	306.71	306.147	-7.04	307.02	307.013	-0.08	305.66	305.765	1.38
7	331.23	330.484	-2.31	332.08	333.21	3.22	328.63	330.706	6.38
8	301.54	301.43	-3.35	300.7	300.461	-10.34	300.02	299.941	-4.41
9	319.26	320.09	3.78	319.22	319.211	-0.04	318.33	315.942	-13.42

and the CFD are in the order of 1/2400.

The high computational efficiency of the methodology developed and the accuracy of the results would seem to indicate the possibility of using the CTFMs developed in conjunction with higher level simulations to eliminate the complexity associated with the smaller scales.

4. Conclusions

A generalised approach to generate reduced order models for compartments, where a mixed convection regime is present, has been presented. The methodology illustrated allows for the generation of accurate thermal fluid network models from validated detailed simulations (CFD models). The CTFM developed utilises interpolated values from the CFD simulations for defining the conductor properties. This is due to the close link which exists in mixed convection between the boundary conditions applied and the flow features developed. For this reason the validity of the CTFM is restricted to the set of boundary conditions defined. The applicability and usefulness of the approach has been shown by modeling a fuselage confined compartment (i.e. crown compartment) and comparing the results with the outcome of CFD simulations.

The methodology developed so far still relies on the researchers experience to find the position and number of nodes to be utilised. The development

of rule base logic tools and their integration in the CFD code, could provide an interesting instrument to automatically define the optimum position and numbers of the nodes. This would be the next step of this research activity but it is at the moment beyond the final aim of this paper.

Acknowledgements

The research leading to these results has received funding from the European Community's Seventh Framework Programme FP7 2007 - 2013 under grant agreement n^o 213371, MAAXIMUS (`www.maaximus.eu`).

References

[1] B. Shapiro, Creating compact models of complex electronic systems: an overview and suggested use of existing model reduction and experimental system identification tools, IEEE Transactions on Components and Packaging Technologies 26 (2003) 165–172.

[2] J. Rambo, Y. Joshi, Reduced-order modeling of turbulent forced convection with parametric conditions, International Journal of Heat and Mass Transfer 50 (2007) 539–551.

[3] M. Cardoso, L. Durlofsky, Linearized reduced-order models for subsurface flow simulation, Journal of Computational Physics 229 (3) (2010) 681–700.

[4] E. Bache, J. M. Vega, A. Velazquez, Model reduction in the back-step fluid-thermal problem with variable geometry, International Journal of Thermal Sciences 49 (12) (2010) 2376–2384.

[5] C. Lasance, H. Vinke, H. Rosten, K. L. Weiner, A novel approach for the thermal characterization of electronic parts, in: Semiconductor Thermal Measurement and Management Symposium, 1995 SEMI-THERM XI, Eleventh Annual IEEE, 1–9, 1995.

[6] C. Lasance, Two benchmarks to facilitate the study of compact thermal modeling phenomena, Components and Packaging Technologies, IEEE Transactions on 24 (4) (2001) 559–565.

[7] E. G. T. Bosch, M. N. Sabry, Thermal compact models for electronic systems, in: Semiconductor Thermal Measurement and Management, 2002. Eighteenth Annual IEEE Symposium, 21–29, 2002.

[8] M. Sabry, Compact thermal models for electronic systems, IEEE Transactions on Components and Packaging Technologies 26 (1) (2003) 179–185.

[9] M. N. Sabry, Compact thermal models for internal convection, IEEE Transactions on Components and Packaging Technologies 28 (1) (2005) 58–64.

[10] M. Sabry, Generalization of the Heat Transfer Coefficient Concept for System Simulation, Journal of Heat Transfer 133 (6) (2011) 060905.

[11] M. Miana, C. Cortes, J. L. Pelegay, J. R. Valdes, T. Putz, Transient Thermal Network Modeling Applied to Multiscale Systems. Part I: Definition and Validation, IEEE Transactions on Advanced Packaging 33 (4) (2010) 924–937.

[12] M. Miana, C. Cortes, J. L. Pelegay, J. R. Valdes, T. Putz, M. Moczala, Transient Thermal Network Modeling Applied to Multiscale Systems. Part II: Application to an Electronic Control Unit of an Automobile, IEEE Transactions on Advanced Packaging 33 (4) (2010) 938–952.

[13] O. Laguerre, S. Benamara, D. Remy, D. Flick, Experimental and numerical study of heat and moisture transfers by natural convection in a cavity filled with solid obstacles, International Journal of Heat and Mass Transfer 52 (25-26) (2009) 5691–5700.

[14] J. Zhang, A. Gupta, J. Baker, Effect of Relative Humidty on the Prediction of Natural Convection Heat Transfer Coefficients, Heat Transfer Engineering 28 (4) (2007) 335–342.

[15] G. D. McBain, Natural convection with unsaturated humid air in vertical cavities, International Journal of Heat and Mass Transfer 40 (13) (1997) 3005–3012.

[16] P. J. Roache, Quantifivation of Uncertainity in Computational Fluid Dynamics, Annual Review Fluid Mechanics 29 (60) (1997) 123–158.

[17] L. F. Richardson, The deferred approach to the limit, Trans. R. Soc. London Ser. A (226) (1927) 229–361.

[18] B. A. Cullimore, C. M. Beer, D. A. Johnson, Propulsion applications of the NASA standard general purpose thermohydraulic analyzer, AIAA 3723.

[19] B. A. Cullimore, S. G. Ring, D. A. Johnson, General Purpose Thermal/Fluid Network Analyzer V5.5, C&R Technologies, Inc., 2011.

[20] D. C. Montgomery, Design and Analysis of Experiments, John Wiley & Sons, 8th edn., 2012.

[21] Ansys Fluent User's Guide, Ansys Inc., Canonsburg, PA, USA, 13.0 edn., 2010.